JOURNAL OF CATALYSIS 125, 285–291 (1990)

Thermal Desorption and Infrared Studies of Amines Adsorbed on SiO_2, Al_2O_3, Fe_2O_3, MgO, and CaO

III. Aniline and *t*-Butylamine

ROLF SOKOLL AND HARTMUT HOBERT

Sektion Chemie der Friedrich-Schiller-Universität, Lessingstrasse 10, 6900 Jena, German Democratic Republic

Received July 7, 1989; revised Feburary 13, 1990

The adsorption of aniline and *t*-butylamine on Al_2O_3, Fe_2O_3, SiO_2, MgO, and CaO at the solid/vapour interfaces has been studied by infrared spectroscopy and temperature-programmed desorption (TPD). At beam temperature the surface complexes formed are the same as those discussed earlier in the case of other amines: there is hydrogen bonding and dissociative adsorption on SiO_2, and formation of coordination bonds between amine molecules and Lewis-acidic surface sites on the other oxides. With increasing temperature during the TPD runs, in the case of aniline only aniline itself desorbs, whereas when *t*-butylamine is used, in addition to the unchanged amine, isobutene and NH_3 can be detected as desorption products, indicating the occurrence of CN bond breakage. With both amines oxidation reactions take place on the surface of Fe_2O_3.

INTRODUCTION

Part I of this series is concerned with the adsorption on oxides of diethylamine and triethylamine (*1*), and Part II reported on isopropylamine and cyclohexylamine (*2*). Chemical transformations of the adsorbed amine molecules with increasing temperatures were studied. With primary aliphatic amines the main high-temperature reaction on oxides possessing Lewis-acidic surface centres is nitrile formation, but secondary aliphatic amines additionally show CN bond breakages causing desorption of NH_3 and propylene (isopropylamine), cyclohexene (cyclohexylamine) as dehydrogenation (cyclohexylamine → aniline; isopropylamine → adsorbed imine species), and CC bond breakage (isopropylamine: adsorbed imine species → desorption of CH_4 and acetonitrile). This paper reports our results with aniline and *t*-butylamine, i.e., molecules with the NH_2 group located on carbon atoms to which no hydrogen is attached.

EXPERIMENTAL

The oxides and their pretreatments were as described in Parts I and II (*1*, *2*). Details of the infrared (IR) and temperature-programmed desorption (TPD) equipment and methods are also given in the previous papers (*1*, *2*).

RESULTS

The IR results are presented in Tables 1 and 3, and in Figs. 2, 3, 5 and 6. The TPD results are given in Figs. 1 and 4, and in Tables 2 and 4.

Tables 1 and 3 list the most important infrared bands of both amines after adsorption on the various oxides and subsequent evacuation at beam temperature (absorptions, not informative for the adsorption process are not discussed in detail; e.g., Al_2O_3/aniline: 3068, 3037 cm^{-1} = ν(=CH) and 1467 cm^{-1} = ν(C=C) (Fig. 2); Al_2O_3/t-butylamine: 2961, 2870 cm^{-1} = $\nu(CH_3)$ and 1472, 1368 cm^{-1} = $\delta(CH_3)$ (Fig. 5); Fe_2O_3/t-

0021-9517/90 $3.00

TABLE 1

Wavenumbers (cm^{-1}) of Infrared Bands of Gaseous Aniline, of Aniline after Adsorption on Oxides at Beam Temperature, and of Adsorbed Reaction Products Formed at Elevated Temperatures

Wavenumber (cm^{-1})						Assignment
Gaseous aniline	SiO_2	CaO	MgO	Fe_2O_3	Al_2O_3	
—	3629	—	—	—	—	ν(OH)/π-interaction
3484	3388	3359	3357	3320	3318	$\nu_{as}(NH_2)$
3406	3319	3293	3292	3248	3246	$\nu_s(NH_2)$
1619	—	—	—	—	—	$\delta(NH_2)$[a]
1624	1598	1595	1595	1593	1591	ν(C=C)[b]
1498	1494	1490	1490	1488	1486	ν(C=C)
—	—	—	—	1436	—	CO_3^{2-}

[a] $\delta(NH_2)$ of adsorbed aniline is partly masked by the (C=C) band.

[b] Band located in the same frequency range, for which reason an exact wavenumber cannot be given.

butylamine: 1464, 1363 cm^{-1} = $\delta(CH_3)$ (Fig. 6, curve II)). Included are also bands of adsorbed reaction products formed at elevated temperatures.

The main interactions between aniline and *t*-butylamine, respectively, and the various oxides which can be detected at beam temperature are the same as those previously discussed in the case of diethylamine (*1*). However, there are new features which provide information about the individual properties of aniline and *t*-butylamine which deserve to be highlighted.

Aniline

With the exception of the oxidation of some adsorbed aniline molecules on Fe_2O_3 and the resulting desorption of CO_2 and H_2O (TPD maximum F IV in Fig. 1: 718 K) there is no case where decomposition prod-

TABLE 2

Adsorption of Aniline on Oxides: Distribution of the Temperature-Programmed Desorption Products

Desorption product	Temperature of the desorption maximum (K)				
	SiO_2	CaO	MgO	Fe_2O_3	Al_2O_3
Aniline	413 658	423	423	433 553 (sh)[a]	443 603 (sh)[a]
Carbon dioxide	—	—	—	718	—
Water	—	—	—	693	—

[a] (sh), shoulder in the TPD curve.

TABLE 3

Wavenumbers (cm^{-1}) of Infrared Bands of Gaseous *t*-Butylamine, of *t*-Butylamine after Adsorption on Oxides at Beam Temperature, and of Adsorbed Reaction Products Formed at Elevated Temperatures

Wavenumber (cm^{-1})				Assignment
Gaseous *t*-butylamine	SiO_2	Al_2O_3	Fe_2O_3	
—	3411	—	—	ν(NH)/sec. amine
3395	3348	3290	3292	$\nu_{as}(NH_2)$
3323	3285	3202	3213	$\nu_s(NH_2)$
—	—	3102	3111	$2\delta(NH_2)$
1616	1584	1570	1576	$\delta(NH_2)$
—	—	—	1547	$\nu_{as}(COO^-)$
—	—	—	1435	$\nu_s(COO^-)$

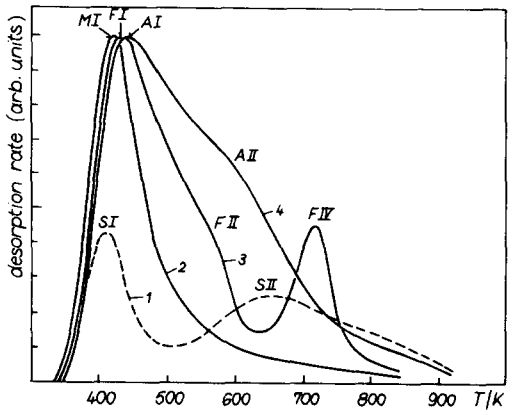

FIG. 1. Thermal desorption curves of aniline adsorbed on oxides at room temperature. (1) SiO_2, (2) MgO, (3) Fe_2O_3, (4) Al_2O_3.

TABLE 4

Adsorption of *t*-Butylamine on Oxides: Distribution of the Temperature-Programmed Desorption Products

Desorption product	Temperature of the desorption maximum (K)		
	SiO_2	Al_2O_3	Fe_2O_3
t-butylamine	403 703	443	433
Isobutene	843	598	573
Ammonia	843	598	573
Carbon dioxide	—	—	638 688
Water	—	—	638 (688)[a]

[a] Small amount.

ucts indicating further chemical transformations can be detected by mass spectrometry. Thus there is no evidence for the formation of diphenylamine on Al_2O_3, as was described in the literature (*3–5*). The consequence of this desorption of unchanged aniline is that in each case, instead of a distinct second TPD maximum, only shoulders (Al_2O_3: ca. 603 K; Fe_2O_3: ca. 553 K) and tails (MgO, CaO), respectively, appear in Fig. 1 on the high-temperature side of the first TPD maximum (as a result of reactions at least two product molecules would be formed from one adsorbed amine molecule, and a higher pressure increase would result in the gas phase; i.e., a more distinct TPD maximum would be caused than in the case of a 1 : 1 desorption).

IR spectra recorded at increased temperatures of the system aniline/Al_2O_3 show no changes of number and frequency of all absorptions already visible at beam temperature (Fig. 2). The intensities of the main bands between 1700 and 1200 cm^{-1} (1591, 1486 cm^{-1}: ν(C=C) of the aromatic ring) merely diminish to a different degree with increasing temperature ($\Delta I(1591) > \Delta I(1486)$). The NH_2 deformation mode of adsorbed aniline is not resolvable (possibly visible as a shoulder at ca. 1570 cm^{-1} after evacuation at 603 K) and yields an asymmetric (on the low-frequency side) absorption together with the ν(C=C) band at 1591 cm^{-1}. Basically the same phenomena appear in the infrared spectra of aniline on MgO and CaO.

With SiO_2 the appearance of the TPD maximum S II (Fig. 1, 658 K) reveals dissociative adsorption of aniline on strained siloxane bridges (because of the desorption of only unchanged aniline the usually observable distinct TPD maximum S III becomes apparent as a long tail on S II at

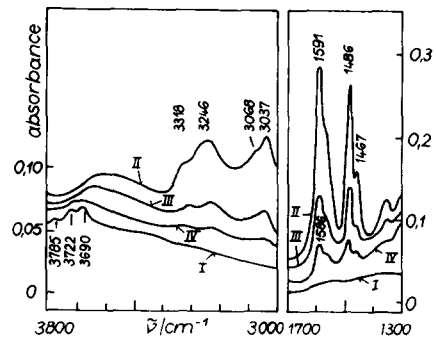

FIG. 2. Infrared spectra of Al_2O_3: (I) under vacuum; (II–IV) after adsorption of aniline from the vapour phase and subsequent evacuation at (II) beam temperature, (III) 533 K, (IV) 603 K.

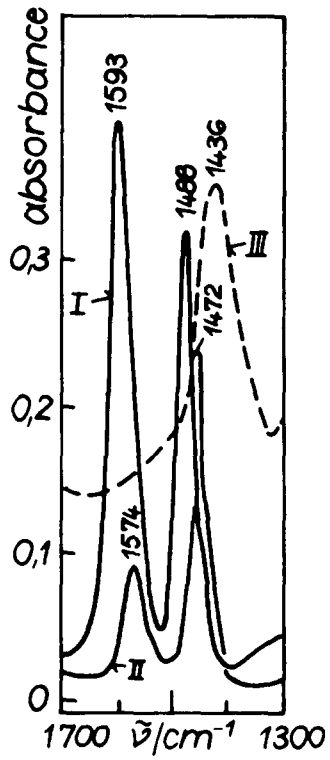

FIG. 3. Difference spectra: (I) = (2) − (1); (II) = (3) − (1); (III) = (4) − (1). Infrared spectra of Fe_2O_3: (1) under vacuum; (2–4) after adsorption of aniline from the vapour phase and subsequent evacuation at (2) beam temperature, (3) 553 K, (4) 603 K.

higher temperatures) (*6*). After evacuation at ca. 573 K, however, the infrared spectra show no NH band of the corresponding secondary amine structure, but only weak (=CH) and (C=C) absorptions of the aromatic ring. As in the case of other aromatic amines a broad band appears additionally at 3629 cm^{-1}.

After adsorption of aniline on Fe_2O_3 and subsequent heating, the IR spectra show mainly the same changes as those in the case of Al_2O_3. However, contrary to Al_2O_3 (beam temperature → 603 K: 1591 → 1586 cm^{-1} and 1486 → 1486 cm^{-1}) on Fe_2O_3 shifts of the (C=C) absorptions to lower wavenumbers are considerably greater (beam temperature → 553 K: 1593 → 1574 cm^{-1} and 1488 → 1472 cm^{-1}), thus indicating a possible change in the surface complex (Fig. 3). This phenomenon does not include oxidation processes, because only an additional temperature increase up to ca. 603 K causes a loss of spectral transmission which is accompanied by the appearance of a new infrared band at 1436 cm^{-1} and by the beginning of the desorption of CO_2 and H_2O.

t-Butylamine

In this case adsorption experiments were performed only with SiO_2, Al_2O_3, and Fe_2O_3 as adsorbents. The following experimental findings reflect the specialities of the interaction between *t*-butylamine and the oxides.

(a) Contrary to many other amines, in addition to oxidation on Fe_2O_3 only one reaction occurs for *t*-butylamine molecules coordinatively bonded to strong Lewis acid sites of Fe_2O_3 and Al_2O_3, and this leads to the desorption of isobutene and NH_3 in the temperature range of TPD maxima F II and A II, respectively (Fig. 4). Thus, with increasing temperature the infrared spectra of *t*-butylamine/Al_2O_3 system show a continuous decrease in the intensity of all bands of adsorbed amine, but no new absorptions of intermediate products can be detected (Fig. 5). Thermal degradation of the secondary

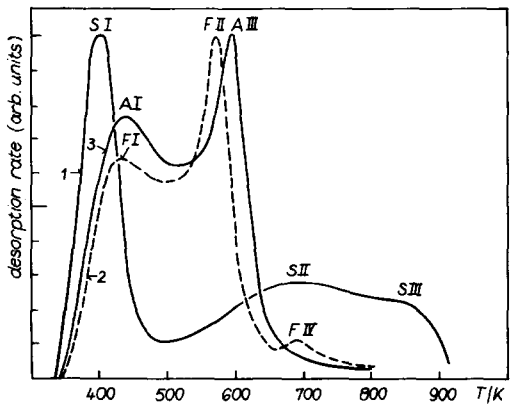

FIG. 4. Thermal desorption curves of *t*-butylamine adsorbed on oxides at room temperature: (1) SiO_2, (2) Fe_2O_3, (3) Al_2O_3.

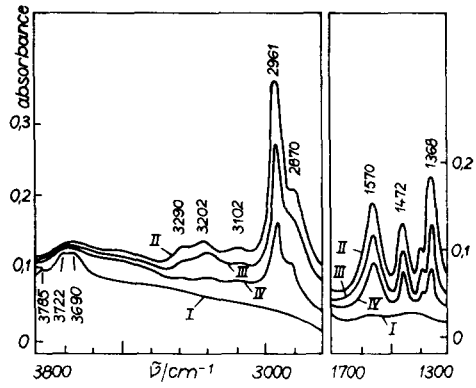

FIG. 5. Infrared spectra of Al_2O_3: (I) under vacuum; (II–IV) after adsorption of *t*-butylamine from the vapour phase and subsequent evacuation at (II) beam temperature, (III) 473 K, (IV) 553 K.

amine structure formed by dissociative adsorption of *t*-butylamine on SiO_2 also leads to the desorption of isobutene and NH_3 in the TPD maximum S III temperature range in Fig. 4 (in addition to the foregoing desorption of unchanged *t*-butylamine in S II, also starting from the secondary amine structure).

(b) Compared to all other aliphatic amines, oxidation of *t*-butylamine on Fe_2O_3 begins at higher temperatures (ca. 503–523 K). This is illustrated by Fig. 6, showing the IR spectra for *t*-butylamine/Fe_2O_3 (curve II) and *n*-butylamine/Fe_2O_3 (curve I) after adsorption at beam temperature and subsequent evacuation at 503 K. In the case of *n*-butylamine, strong carboxylate bands are fully developed (1537, 1414 cm^{-1}), whereas with *t*-butylamine the corresponding absorptions (1547, 1435 cm^{-1}) appear only as weak shoulders.

(c) The second TPD maximum of the system *t*-butylamine/Fe_2O_3 (F II in Fig. 4) appears at 578 K (between 513 and 523 K with the other investigated aliphatic amines), thus covering the first desorption maximum of CO_2 and H_2O at ca. 638 K. Therefore only one separate desorption maximum of oxidation products can be detected at 688 K.

DISCUSSION

Aniline

Contrary to all other investigated amines in the case of aniline only unchanged aniline itself desorbs during TPD runs up to the highest reached temperatures. This is confirmed by other TPD experiments, e.g., under a flow of nitrogen (aniline/Al_2O_3 (*7*)), and can be attributed to the strong CN bond in aniline (D_{CN} = 435 kJ/mol (*8*)) which does not allow the abstraction of NH_3 found in the case of *t*-butylamine (D_{CN} = 352 kJ/mol). Thus with increasing temperature a successive desorption of aniline occurs from Al_2O_3, beginning with the most weakly bonded molecules (adsorbed on weak Lewis acid sites). This is also indicated by the infrared spectra, because the stronger intensity loss of the ν(C=C) at 1591 cm^{-1} (*X*) compared to that of the ν(C=C) at 1486 cm^{-1} (*Y*) shows that aniline molecules remaining on the oxide surface at a fixed temperature are bonded to stronger Lewis acid sites than those of molecules already desorbed. Other literature data confirm this conclusion. Thus by treat-

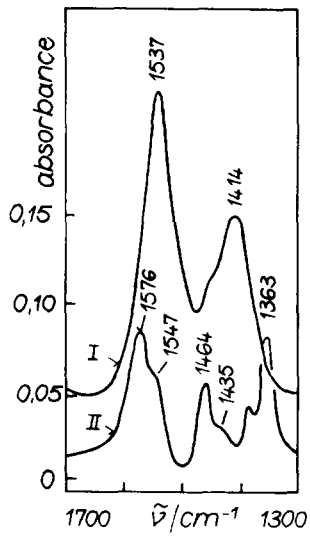

FIG. 6. Infrared spectra of Fe_2O_3 after adsorption of amines at beam temperature and subsequent evacuation at 503 K: (I) *n*-butylamine; (II) *t*-butylamine.

ment of Al_2O_3 with HCl, stronger Lewis acid centres are generated at the solid surfaces (*9, 10*), and after subsequent adsorption of aniline the intensity ratio of the two bands (I_X/I_Y) is remarkably smaller than that in the case of untreated Al_2O_3. Obviously this intensity ratio depends on the degree of demand of the free electron pair on the N atom by the bond formation with interaction partners. This conclusion can also be drawn from the infrared spectra of different compounds (e.g., I_X/I_Y of liquid aniline is greater than that in the case of the coordination compound $C_6H_5NH_2 \cdot BF_3$ (*11*)). Our results concerning the adsorption of aniline on SiO_2 agree with existing literature data (*12–14*). However, in addition to the formation of hydrogen bonds between aniline and surface hydroxy groups of SiO_2 as the main interaction, we found by the TPD curves that dissociative adsorption also occurs analogous to all other NH-containing amines (*6*). In the case of aniline the latter was not described up to now by other authors, probably because of the low intensity and the lack of unambiguousness of the corresponding IR spectroscopic features. Finally the broad absorption at ca. 3629 cm^{-1} can be attributed to a ν(OH) band of surface hydroxy groups of SiO_2 interacting with the π-system of adsorbed aniline molecules, thus showing the existence of a dual-site interaction (*15*).

In the case of the aniline/Fe_2O_3 system during the TPD runs a phenomenon can be observed which seems to be characteristic for all aromatic compounds adsorbed on Fe_2O_3. This is the fact that, compared to that of aliphatic amines, desorption of the products of deep oxidation (CO_2, H_2O) begins at higher temperatures and shows only one maximum (718 K). This is probably caused again by the high stability of the aromatic system which allows the initial steps of oxidation (H-abstraction and/or breakage of the bond between the carbon atom and the functional group) to occur only under more drastic reaction conditions. Thus investigations of catalytic oxidation of hydrocarbons (alkanes, alkenes, alkynes, aromatic hydrocarbons) showed that aromatic hydrocarbons are oxidized with most difficulty (*16*). In our case the mechanism of the oxidation reaction is not clear. From the literature it is known that aniline reacts finally to *p*-benzoquinone in acidic solution; benzene yields the same product in metal-containing solutions, and oxidation of gaseous benzene over, e.g., Fe_2O_3 catalysts leads mainly to the formation of CO_2 (benzene → phenol → quinone → maleic anhydride → CO_2) (*17*). With the exception of CO_2 none of these products can be detected in our experiments, but the infrared band at 1436 cm^{-1} appearing from ca. 603 K refers to a formation of symmetrical carbonate on the Fe_2O_3 surface which then should be the precursor of the CO_2 desorption.

t-Butylamine

As in the case of aniline, formation of imine or nitrile species, respectively, by dehydrogenation is not possible with *t*-butylamine. Therefore only one high-temperature reaction occurs on all oxides investigated; this consists of a CN bond breakage and leads to the desorption of NH_3 and isobutene. In the case of Al_2O_3 and Fe_2O_3 the intermediate products of this process can be ionic in nature, analogous to the proposed elimination mechanism for the catalytic dehydrochlorination of *t*-butyl chloride (*18*). Contrary to all other investigated amines, in the case of the *t*-butylamine/Fe_2O_3 system very small amounts of oxidation products desorb at 638 and 688 K, and using Al_2O_3 as adsorbent formation of surface carboxylates (*1*) does not occur. These phenomena show that *t*-butylamine can be oxidized only with great difficulty (resulting from the structure of the molecule), which is in accordance with data concerning the catalytic oxidation of isobutene and *t*-butyl alcohol (*19*).

CONCLUSIONS

The results presented show that adsorption of *t*-butylamine and aniline on oxides leads to the formation of surface complexes at beam temperature which are identical

with those in the case of diethylamine and isopropylamine (*1, 2*). However, differences exist with regard to the surface reactions initiated at elevated temperatures during the TPD runs. Thus, formation of corresponding imine and nitrile species, respectively, which always occurs in the case of all amines investigated up to now (*1, 2*), is not possible using amines with the NH_2 group located on carbon atoms to which no hydrogen is attached. In addition to oxidation on Fe_2O_3 only one high-temperature reaction can be detected of *t*-butylamine molecules coordinatively bonded to strong Lewis acid sites of oxides; this consists of the breakage of CN bonds and leads to the desorption of NH_3 and isobutene. Furthermore, *t*-butylamine can be fully oxidized only with difficulty, because C–C bond breakage is necessary. The strong CN bond in aniline does not allow the abstraction of NH_3, and therefore only unchanged aniline itself desorbs during the TPD runs. Products of deep oxidation in the system aniline/Fe_2O_3 can be detected only at higher temperatures as in the case of aliphatic amines, probably as a result of the high stability of the aromatic ring.

REFERENCES

1. Sokoll, R., Hobert, H., and Schmuck, I., *J. Catal.*, **121,** 153 (1990).
2. Sokoll, R., Hobert, H., and Schmuck, I., *J. Catal.*, submitted for publication [Part II].
3. Hoelscher, H. E., and Chamberlain, D. F., *Ind. Eng. Chem.* **42,** 1558 (1950).
4. Rieche, A., and Möller, R., *J. Prakt. Chem.* **15,** 24 (1962).
5. Pasek, J., *Collect. Czech. Chem. Commun.* **28,** 1007 (1963).
6. Rudakoff, G., Sokoll, R., Hobert, H., and Schmuck, I., *Z. Chem.* **27,** 150 (1987).
7. Ogasawara, S., Takagawa, M., and Takahashi, K., *J. Catal.* **29,** 67 (1973).
8. Weast, R. C., "Handbook of Chemistry and Physics," 64th ed. CRC Press, Boca Raton, FL, 1984.
9. Khalafalla, S. E., and Haas, L. A., *J. Catal.* **24,** 115 (1972).
10. Baumgarten, E., and Zachos, A., *Spectrochim. Acta Part A* **37,** 757 (1981).
11. Tanaka, M., and Ogasawara, S., *J. Catal.* **25,** 111 (1972).
12. Low, M. J. D., and Hasegawa, M., *J. Colloid Interface Sci.* **26,** 95 (1968).
13. Low, M. J. D., and Subba Rao, V., *Canad. J. Chem.* **47,** 1281 (1969).
14. Oranskaja, O. M., Filimonov, V. N., and Schmuljakovski, Ya. E., *Usp. Fotoniki* **4,** 74 (1974).
15. W. Pohole, *J. Chem. Soc. Faraday Trans. 1* **78,** 2101 (1982).
16. Stein, K. C., Freenan, J. J., Thompson, G. P., Shultz, J. F., Hofer, L. J. E., and Anderson, R. B., *Ind. Eng. Chem.* **52,** 671 (1960).
17. Germain, J.-E., and Laugier, R., *Bull. Soc. Chim. Fr.*, 2910 (1972).
18. Ueda, W., Hiraiwa, J., Yoshida, N., and Kishimoto, S., *Ber. Bunsengers. Phys. Chem.* **90,** 353 (1986).
19. Tan, S., Moro-Oka, Y., and Ozaki, A., *J. Catal.* **17,** 132 (1970).